

Supporting Information

Selective gas adsorption properties of microporous metal-organic frameworks with active Lewis basic sites: experimental and theoretical study

S.A. Sapchenko, D.N. Dybtsev, D. G. Samsonenko, R.V. Belosludov, V. Belosludov,
Y. Kawazoe, M. Schröder and V.P. Fedin

General remarks

All chemicals purchased were of reagent grade and were used as received without further purification. FTIR spectra (KBr pellets) were recorded in range 4000–400 cm^{-1} on a Scimitar FTS 2000 Fourier-transform infrared spectrometer. Powder X-ray diffraction (PXRD) data were collected with Cu- K_{α} radiation on a Phillips PW 1830 instrument equipped with a PW 1820 vertical Bragg-Bretano powder goniometer and a PW 1710 control unit. Thermogravimetric analysis was carried out on a TG 209 F1 thermobalance (Netzsch); the samples were heated in an atmosphere of a nitrogen/oxygen mixture with a heating rate of 10 $\text{deg}\cdot\text{min}^{-1}$. Elemental analyses on C, H and N were performed on the Euro EA 3000 CHN Elemental Analyzer. The synthesis of **1s** was carried out according to the reported procedure [1].

Synthesis of $[\text{Zn}_{11}(\text{H}_2\text{O})_2(\text{ur})_4(\text{bpdc})_{11}]\cdot 7\text{DMF}$ (**2s**) and $[\text{Zn}_{11}(\text{H}_2\text{O})_2(\text{ur})_4(\text{bpdc})_{11}]$ (**2**)

A mixture of $\text{Zn}(\text{ClO}_4)_2\cdot 6\text{H}_2\text{O}$ (0.300 g, 0.80 mmol), 4,4'-biphenyldicarboxylic acid (0.240 g, 1.00 mmol), urotropine (0.280 mg, 2 mmol) and DMF (25 ml) was mixed, sonicated for a half of an hour and heated at 100°C for 1 hour in a sealed glass vessel, afterwards the liquid phase was parted from the solid residue by centrifugation and heated for another 4 hours. The obtained colorless prismatic crystals of **2s** were filtered, washed with DMF and dried upon air. Yield 0.154 g (47% based on Zn). Anal. calcd. for $\text{C}_{199}\text{H}_{189}\text{N}_{23}\text{O}_{53}\text{Zn}_{11}$ (%): C 53.5; H 4.3; N 7.2. Found (%): C 53.8; H 4.4; N 7.3. The phase purity of **2s** was confirmed by powder X-ray diffraction data (Fig. S1).

Stability in different solvents. According to powder X-ray diffraction data, the solvated crystalline compound **2s** is not stable in some organic solvents such as CH_2Cl_2 , acetone or benzene. Treatment of **2s** with cyclohexene does not seem to affect its crystallinity except for some acceptable rearrangements in the intensities of reflections. Also, exposure of **2s** to open atmosphere for several days results in a deterioration of the framework (see Fig. S2).

Activation procedure. The crystals of **2s** were soaked in cyclohexane for 3 days, thereupon dried and heated in dynamic vacuum at 50°C over night. The obtained compound **2** was used in gas

sorption experiments. Anal. calcd. for $C_{178}H_{140}N_{16}O_{46}Zn_{11}$ (%): C 54.0; H 3.6; N 5.7. Found (%): C 54.5; H 3.4; N 5.3. The activated compound retains its crystallinity, according to XRPD (see Fig. S1).

Thermogravimetric studies

The as-synthesised compound **2s** (*ca.* 5 mg) was placed on the thermobalance and gradually heated in the N_2/O_2 stream. The sample weight loss plot is composed of three distinct steps (Fig. S3): the first one in the temperature range 25 —200°C is attributed to the release of solvent molecules (DMF + H_2O), the second small step (200—300°C) is the release of urotropine molecules, the third step (400—500°C) is related to the pyrolysis of the biphenyldicarboxylate ligands of the framework.

Crystallographic studies

Single-crystal X-ray diffraction data of **2s** were collected at 90 K using synchrotron radiation at Beamline 2D: Supramolecular Crystallography (Pohang Accelerator Laboratory, Pohang, South Korea), equipped with one-circle goniometer and the ADSC Quantum 210 two-coordinate detector ($\lambda = 0.90000 \text{ \AA}$, silica monochromator, ϕ scanning). Data collecting, frame integration and processing the reflexes array with calculation the crystal's absorption were performed using HKL2000 program [2]. The structures were solved by direct methods and refined on F^2 by full-matrix least-squares technique in the anisotropic approximation (for non-hydrogen atoms) using SHELX-97 program package [3]. Positions of the hydrogen atoms of 4,4'-biphenyldicarboxylate and urotropin ligands were calculated geometrically and refined by the rigid model. The crystallographic data and details of the structure refinements are summarized in Table S1. Selected interatomic distances are given in Table S2. The Cambridge Crystallographic Data Centre deposition number is CCDC 1059061.

Gas adsorption studies

The sorption isotherms for N_2 , CO, CO_2 and C_2H_2 in **1** and **2** were measured on BELSORP-max instrument using high-purity gases in the range of 0.0–1.0 bar at 77 K for N_2 (liq. N_2 bath), 273 (ice bath) and 298 K (water bath) for CO, CO_2 , C_2H_2 respectively. Prior to the experiment the samples were degassed under dynamic vacuum at 45°C for 1 h. The N_2 adsorption isotherms for **2** are provided on Fig. S3. The surface area was calculated by the multipoint BET method in the range of $p/p_0 < 0.15$.

The experimental sorption data were fitted by a virial equation:

$$\ln p = \ln n + 1/T(a_0 + a_1n + a_2n^2 + a_3n^3) + b_0 + b_1n + b_2n^2,$$

where p is pressure (normalized to $p_0=1$ bar), n is coverage (mol g⁻¹), T is temperature, and a_i and b_i are temperature independent empirical parameters. Their values for each investigated gas are given in Table S3.

Henry's constants K_H were determined as functions of temperature:

$$K_H = \exp(-a_0/T - b_0)$$

The selectivity factors SF(X/Y) for gas X over gas Y at given temperature T were determined as the ratio of Henry's constants at corresponding T:

$$SF_T(X/Y) = K_{H,T}(X)/K_{H,T}(Y).$$

The isosteric heat of adsorption was determined as a function of coverage:

$$Q_{st} = -R(a_0 + a_1n + a_2n^2 + a_3n^3).$$

The values of the Henry's constants and selectivity factors for binary mixtures of CO, CO₂ and C₂H₂ calculated for **1** and **2** are given in Tables S4 and S5.

Table S6 summarizes the reported CO₂/CO selectivity factors, calculated as the Henry's constants ratios at ambient temperature with the corresponding numbers for **1** and **2**.

IAST calculations

The ideal adsorbed solution theory (IAST) calculations were performed in order to estimate the corresponding selectivity factors at different temperatures and absolute pressures.

The experimental sorption plots of pure i -component were approximated by a continuously differentiable function

$$F_i(p) = Ap_i \exp(kp_i + k_0) + Bp_i + C.$$

The relationship between P , y_i and x_i (P = the total pressure of the gas phase, y_i = mole fraction of the i -component in gas phase, x_i = mole fraction of the i -component in adsorbed state) was written according to the IAST theory [12]:

$$\int_{p=0}^{p=\frac{Py_1}{x_1}} F_1(p) d \ln p = \int_{p=0}^{p=\frac{Py_2}{x_2}} F_2(p) d \ln p .$$

The given relationship allowed us to calculate the relationship between the selectivity factor of the stronger absorbed component over less strongly absorbed component in the binary mixtures of the investigated gases and the overall pressure at the given temperature. The selectivity factor was determined as:

$$s_{1/2} = \frac{y_1/x_1}{y_2/x_2} .$$

The relationship between molar fractions of the component in the absorbed state and in the gas phase at two temperatures (273, 298 K) and overall gas pressure $p = 1$ bar was defined (Fig. 3 in the main text). Also, the dependencies of the selectivity factors on the total pressure of the gas phase for the equimolar mixtures of C_2H_2/CO and CO_2/CO were calculated at 273 and 298 K (Fig. S4).

Calculation methods: First-principles calculations were performed within the framework of density functional theory (DFT), as implemented in the Vienna Ab initio Simulation Package (VASP) [13,14]. Electron exchange-correlation was treated by the generalized gradient approximation (GGA) with Perdew, Burke, and Ernzerhof (PBE) parameterization [15], and interactions between the ion cores and valence electrons were modeled by the all-electron projector augmented wave (PAW) method [16,17]. The plain-wave cutoff energy was 400 eV and convergence in energy (10^{-4} eV) and force (5×10^{-3} eV/Å) were used during the optimization procedure. Brillouin zone integrations were performed using the Monkhorst-Pack k-point mesh [18] with a $2 \times 1 \times 3$ grid. In order to properly estimate the weak non-covalent interactions, the energy calculations were carried out using the van der Waals (vdW) corrected exchange correlated DFT potential within the Grimme method [19].

The adsorption energies (E_{ads}) were calculated as the difference between the sum of the binding energies of the empty MOF (E_{host}) and the number of non-coordinated guest molecules ($n \cdot E_{guest}$), with n equal to the number of adsorbed non-coordinated molecules, and that of the adsorbed system ($E_{host+guest}$) and the adsorption state, with a negative value of E_{ads} being thermodynamically favorable [Eq. (1)].

$$E_{ads} = E_{host+guest} - (E_{host} + n * E_{guest}) \quad (1)$$

The interaction between the porous host and the substrate has been demonstrated by a charge density isosurface. The difference in charge density (excess and depletion electrons) was estimated by:

$$\Delta\rho = \rho(\text{host+guest}) - \rho(\text{host}) - \sum_{k=1}^n \rho_k(\text{guest}), \quad (2)$$

and the obtained density results were visualized using the XCrySDen code [20]. The theoretical analysis described above has been verified in previous studies [21-23].

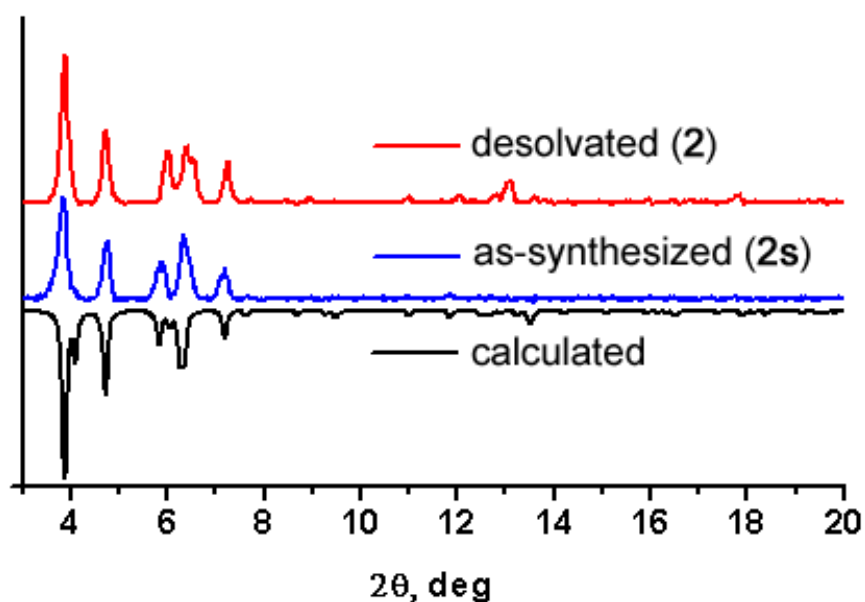


Fig S1. PXRD plots for compounds **2s** and **2** vs. the theoretical plot, calculated for **2s**, based on its single-crystal X-ray diffraction data.

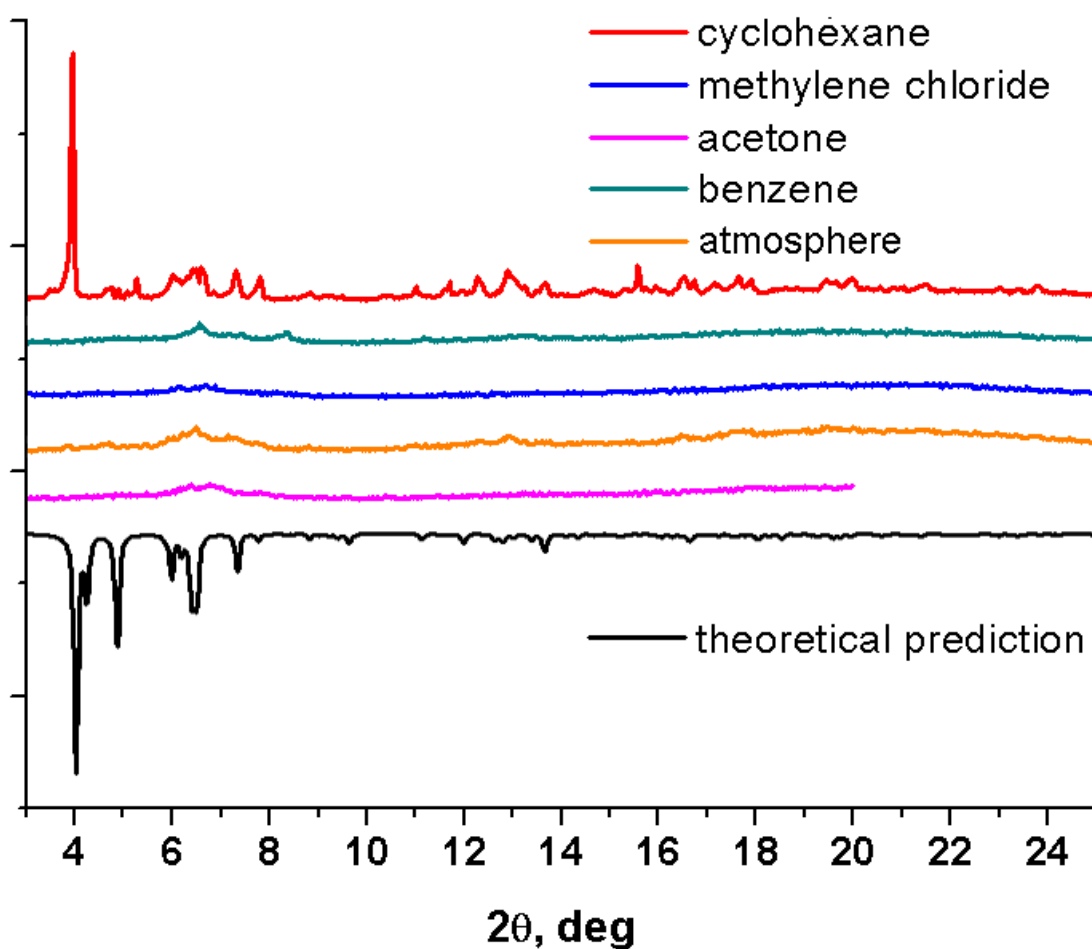


Fig S2. Stability of **2s** in different solvents monitored by powder X-ray diffraction.

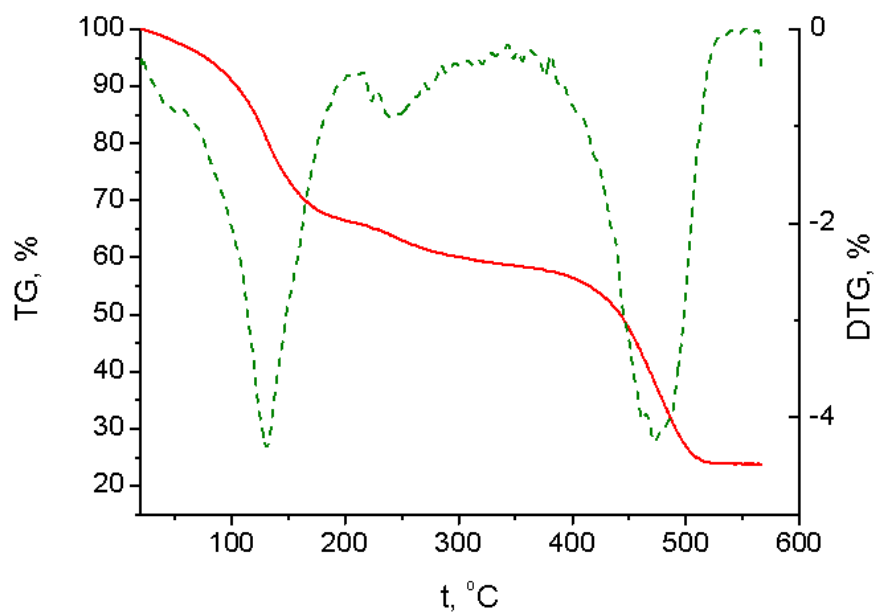


Fig. S3. TG (red) and DTG (green) plots for compound **2s**.

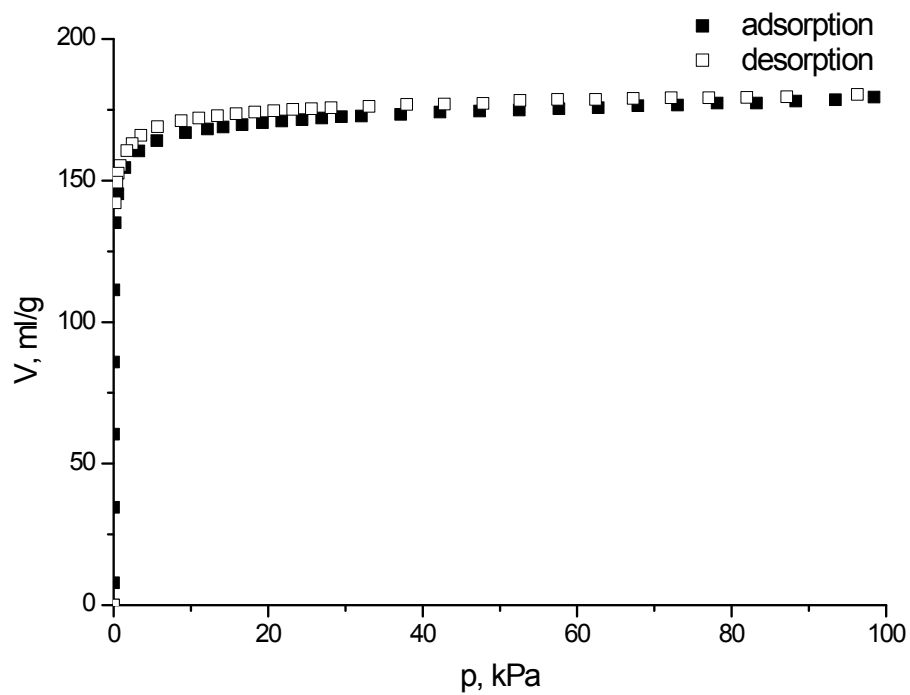


Fig S3. N_2 adsorption/desorption isotherms in **2** recorded at 77 K.

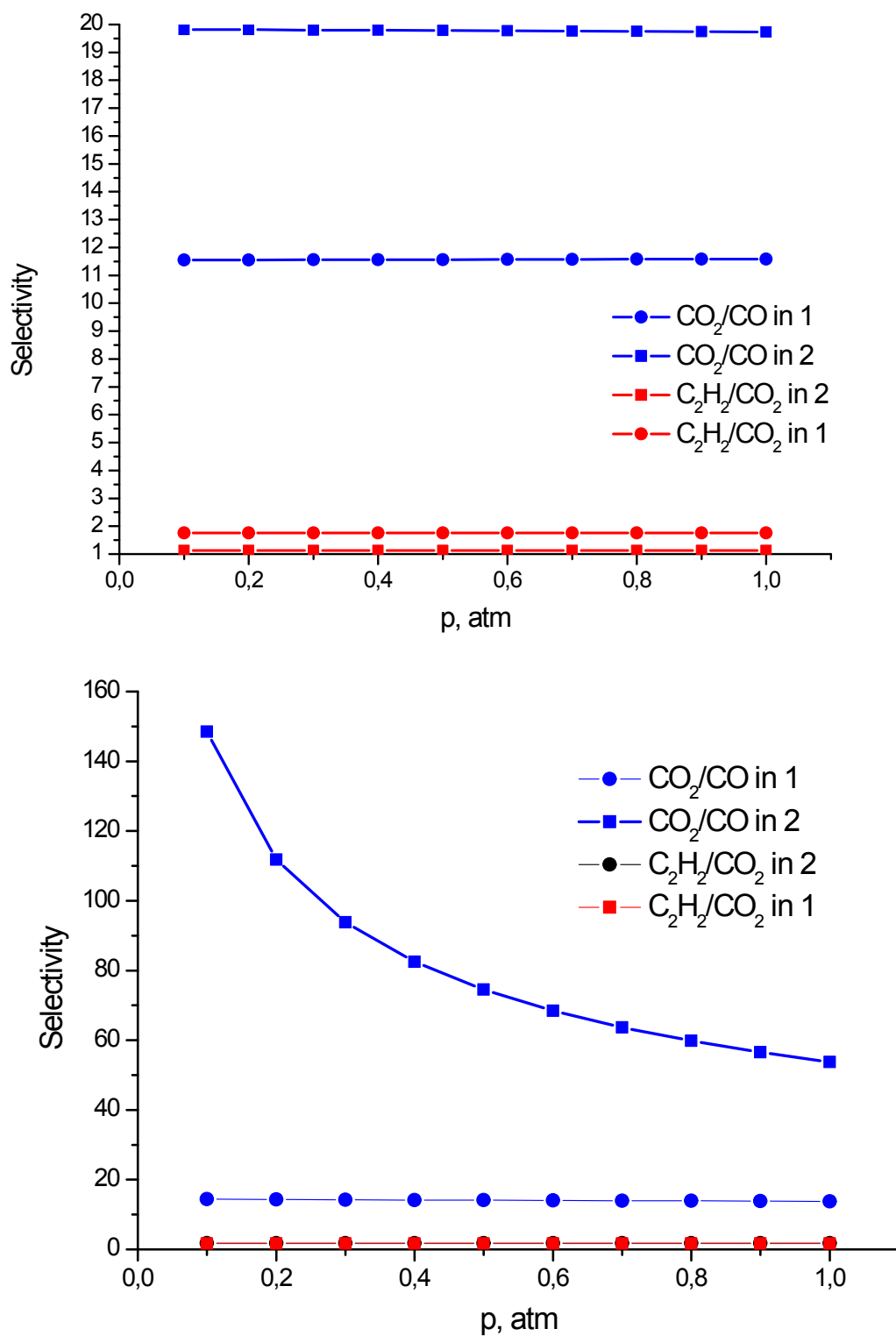


Fig. S5. The dependences of IAST adsorption selectivity for compounds **1** and **2** on the total pressure for CO₂/CO, and C₂H₂/CO₂ mixtures at 273 (top) and 298 K (bottom).

Table S1. Crystal data and structure refinement for **2s**

Identification code	2s
Empirical formula	C ₁₉₉ H ₁₈₉ N ₂₃ O ₅₃ Zn ₁₁
Molar mass, g/mol	4469.80
<i>T</i> , K	90
λ , Å	0.90000
Crystal system	Моноклинная
Space group	<i>P2/c</i>
<i>a</i> , Å	22.018(1)
<i>b</i> , Å	20.783(1)
<i>c</i> , Å	37.062(1)
β , deg.	94.845(1)
<i>V</i> , Å ³	16899.0(12)
<i>Z</i>	2
<i>D</i> _{calcd} , g/cm ³	0.878
μ , mm ⁻¹	1.535
F(000)	4596
Crystal size, mm	0.08 × 0.06 × 0.04
θ range, deg.	1.71–35.25
Limiting indices <i>hkl</i>	$-25 < h < 25$, $-23 < k < 23$, $-47 < l < 47$
Reflections collected/unique	94135 / 29546
<i>R</i> _{int}	0.0646
<i>T</i> _{max} / <i>T</i> _{min}	0.9412 / 0.8871
Goodness-of-fit (GOF) on <i>F</i> ²	1.017
Final <i>R</i> indices [<i>I</i> > 2 σ (<i>I</i>)]	<i>R</i> ₁ = 0.0788, <i>wR</i> ₂ = 0.2235
<i>R</i> -indices (all data)	<i>R</i> ₁ = 0.0912, <i>wR</i> ₂ = 0.2339
Largest difference in peak and hole, e/Å ³	0.904 / -1.572

Table S2. Selected bond lengths and angles for **2s**

Bond	<i>d</i> , Å	Bond	<i>d</i> , Å
Zn(1)-N(11)	2.073(3)	Zn(4)-N(13)	2.092(3)
Zn(1)-O(11)	2.059(3)	Zn(4)-O(24)#4	1.928(4)
Zn(1)-O(21)	1.997(2)	Zn(4)-O(43)#5	1.912(10)
Zn(1)-O(31)	1.988(3)	Zn(4)-O(45)#5	2.181(9)
Zn(1)-O(41)	2.051(3)	Zn(4)-O(46)#5	2.017(7)
Zn(2)-N(21)	2.060(3)	Zn(4)-O(1M)	1.985(6)
Zn(2)-O(12)	2.016(3)	Zn(4)-O(2M)	2.014(7)
Zn(2)-O(22)	2.069(3)	Zn(5)-N(22)	2.072(3)
Zn(2)-O(32)	2.056(3)	Zn(5)-O(14)#1	1.974(2)
Zn(2)-O(42)	1.993(3)	Zn(5)-O(53)#4	2.023(3)
Zn(3)-N(12)	2.062(3)	Zn(5)-O(61)	2.285(3)
Zn(3)-O(51)	2.016(3)	Zn(5)-O(62)	2.059(3)
Zn(3)-O(52)#1	2.023(3)	Zn(6)-O(13)#1	2.053(2)
Zn(3)-O(63)#2	2.011(3)	Zn(6)-O(54)#6	2.023(3)
Zn(3)-O(64)#3	2.027(3)	Zn(6)-O(62)	2.193(3)
Angle	ω , deg.	Angle	ω , deg.
O(11)-Zn(1)-N(11)	98.82(11)	O(24)#4-Zn(4)-O(2M)	86.1(3)
O(21)-Zn(1)-N(11)	100.91(11)	O(43)#5-Zn(4)-N(13)	116.5(4)
O(21)-Zn(1)-O(11)	89.76(12)	O(43)#5-Zn(4)-O(24)#4	97.1(4)
O(21)-Zn(1)-O(41)	88.52(14)	O(43)#5-Zn(4)-O(45)#5	22.0(3)
O(31)-Zn(1)-N(11)	99.57(12)	O(43)#5-Zn(4)-O(46)#5	45.0(4)
O(31)-Zn(1)-O(11)	86.97(13)	O(43)#5-Zn(4)-O(1M)	104.6(4)
O(31)-Zn(1)-O(21)	159.52(12)	O(43)#5-Zn(4)-O(2M)	142.6(4)
O(31)-Zn(1)-O(41)	88.38(14)	O(46)#5-Zn(4)-N(13)	111.9(3)
O(41)-Zn(1)-N(11)	99.15(12)	O(46)#5-Zn(4)-O(45)#5	59.6(3)
O(41)-Zn(1)-O(11)	161.95(13)	O(1M)-Zn(4)-N(13)	103.3(2)
N(21)-Zn(2)-O(22)	101.84(11)	O(1M)-Zn(4)-O(45)#5	121.3(4)
O(12)-Zn(2)-N(21)	100.90(13)	O(1M)-Zn(4)-O(46)#5	61.8(4)
O(12)-Zn(2)-O(22)	91.37(12)	O(1M)-Zn(4)-O(2M)	40.0(3)
O(12)-Zn(2)-O(32)	87.06(15)	O(2M)-Zn(4)-N(13)	89.3(2)
O(32)-Zn(2)-N(21)	96.17(12)	O(2M)-Zn(4)-O(45)#5	161.3(4)
O(32)-Zn(2)-O(22)	161.89(12)	O(2M)-Zn(4)-O(46)#5	101.8(4)
O(42)-Zn(2)-N(21)	100.08(14)	N(22)-Zn(5)-O(61)	93.63(12)
O(42)-Zn(2)-O(12)	158.82(12)	O(14)#1-Zn(5)-N(22)	91.89(11)
O(42)-Zn(2)-O(22)	87.16(14)	O(14)#1-Zn(5)-O(53)#4	116.87(12)
O(42)-Zn(2)-O(32)	87.83(16)	O(14)#1-Zn(5)-O(61)	150.97(13)
O(51)-Zn(3)-N(12)	103.58(11)	O(14)#1-Zn(5)-O(62)	99.31(12)
O(51)-Zn(3)-O(52)#1	88.58(13)	O(53)#4-Zn(5)-N(22)	98.28(13)
O(51)-Zn(3)-O(64)#3	87.68(12)	O(53)#4-Zn(5)-O(61)	90.48(12)
O(52)#1-Zn(3)-N(12)	97.99(11)	O(53)#4-Zn(5)-O(62)	109.29(12)
O(52)#1-Zn(3)-O(64)#3	163.49(11)	O(62)-Zn(5)-N(22)	140.96(12)
O(63)#2-Zn(3)-N(12)	96.26(11)	O(62)-Zn(5)-O(61)	59.99(12)
O(63)#2-Zn(3)-O(51)	160.16(11)	O(13)#1-Zn(6)-O(13)#7	179.995(2)
O(63)#2-Zn(3)-O(52)#1	89.03(12)	O(13)#1-Zn(6)-O(62)	89.55(10)
O(63)#2-Zn(3)-O(64)#3	89.05(12)	O(13)#7-Zn(6)-O(62)	90.45(10)
O(64)#3-Zn(3)-N(12)	98.52(11)	O(54)#4-Zn(6)-O(13)#1	89.38(10)
N(13)-Zn(4)-O(45)#5	97.0(2)	O(54)#6-Zn(6)-O(13)#1	90.61(10)

O(24)#4-Zn(4)-N(13)	127.34(19)	O(54)#4-Zn(6)-O(62)	85.99(12)
O(24)#4-Zn(4)-O(45)#5	103.6(3)	O(54)#6-Zn(6)-O(62)	94.01(12)
O(24)#4-Zn(4)-O(46)#5	120.4(3)	O(62)-Zn(6)-O(62)#3	180
O(24)#4-Zn(4)-O(1M)	106.0(3)		

Symmetry transformations used to generate equivalent atoms: #1 $-x+2, y, -z+3/2$; #2 $x, -y+1, z+1/2$; #3 $-x+2, -y+1, -z+1$; #4 $-x+2, -y, -z+1$; #5 $-x+1, -y, -z+1$; #6 $x, y+1, z$; #7 $x, -y+1, z-1/2$.

Table S3. Results of the fitting the adsorption isotherms of CO, CO₂ and C₂H₂.

gas Parameters	CO	CO ₂	C ₂ H ₂
Compound 1			
a_0	$-1.687805 \cdot 10^3$	$-2.58394 \cdot 10^3$	$-2.885236 \cdot 10^3$
a_1	$6.364091 \cdot 10^4$	$3.551724 \cdot 10^3$	$4.042514 \cdot 10^5$
a_2	$5.946557 \cdot 10^4$	$9.967271 \cdot 10^3$	$-4.763482 \cdot 10^5$
a_3	$5.789381 \cdot 10^3$	$4.894518 \cdot 10^4$	$-1.046584 \cdot 10^6$
b_0	19,49315	20,09169	20.38299
b_1	$-1.862229 \cdot 10^3$	33.00452	$-9.196694 \cdot 10^2$
b_2	$5.137360 \cdot 10^4$	$3.890923 \cdot 10^4$	$-9.712653 \cdot 10^4$
Compound 2			
a_0	$-1.012013 \cdot 10^3$	$-3.287444 \cdot 10^3$	$-2.939391 \cdot 10^3$
a_1	$-1.872655 \cdot 10^4$	$5.723855 \cdot 10^3$	$4.025579 \cdot 10^6$
a_2	$4.039135 \cdot 10^4$	$-5.969325 \cdot 10^3$	$-1.528204 \cdot 10^7$
a_3	-71.55589	$-1.161188 \cdot 10^4$	$2.560586 \cdot 10^7$
b_0	18.38741	23,22848	21,45791
b_1	$-9.545592 \cdot 10^3$	$1.760146 \cdot 10^3$	$-1.054003 \cdot 10^4$
b_2	$1.270045 \cdot 10^4$	$-2.551774 \cdot 10^4$	$-3.34498 \cdot 10^6$

Table S4. Henry constants calculated for **1** and **2**.

Sorbate	Polarizability, (10^{-25} cm^3)	$K_{H, 273}$ (Pa·kg/mol)	$K_{H, 298}$ (Pa·kg/mol)
Compound 1			
CO	19.5	$(1.7 \pm 0.4) \cdot 10^{-6}$	$(1.0 \pm 0.1) \cdot 10^{-6}$
CO ₂	29.1	$(2.7 \pm 0.5) \cdot 10^{-5}$	$(1.1 \pm 0.1) \cdot 10^{-5}$
C ₂ H ₂	39.3	$(5.5 \pm 0.1) \cdot 10^{-5}$	$(2.25 \pm 0.04) \cdot 10^{-5}$
Compound 2			
CO	19.5	$(4.6 \pm 0.7) \cdot 10^{-7}$	$(3.4 \pm 0.5) \cdot 10^{-7}$
CO ₂	29.1	$(1.5 \pm 0.4) \cdot 10^{-5}$	$(5 \pm 1) \cdot 10^{-6}$
C ₂ H ₂	39.3	$(2.5 \pm 0.4) \cdot 10^{-5}$	$(1.0 \pm 0.2) \cdot 10^{-5}$

Table S5. Selectivity factors calculated for **1** and **2**.

	273 K	298 K
Compound 1		
SF(CO ₂ /CO)	15.3	11.2
SF(C ₂ H ₂ /CO ₂)	2.1	2.0
SF(C ₂ H ₂ /CO)	31.5	22.1
Compound 2		
SF(CO ₂ /CO)	32.3	15.8
SF(C ₂ H ₂ /CO ₂)	1.7	1.9
SF(C ₂ H ₂ /CO)	54.1	29.6

Table S6. The comparison of the published CO₂/CO selectivity factors, calculated as the Henry's constants ratios at ambient temperature.

Material	T, K	S(CO ₂ /CO)	Ref.
ZIF-68	273	19.2	5
ZIF-69	273	20.9	
ZIF-70	273	37.8	
MTV-MOF-5-EHI	298	10.2	6
MTV-MOF-5-EI	298	7.6	
MOF-5	298	2.1	
ZIF-100	298	17.3	7
ZIF-95	298	11.4	
[Zn ₂ (L)(H ₂ O)]Cl (L=1,4,7-tris(4-carboxybenzyl)-1,4,7-triazacyclononane)	298	21.1	8
[Zn(BDC)(dabco) _{0.5}]	298	10 *	9
[Zn(BDC-OH)(dabco) _{0.5}]	298	16 *	
OSHC	288	10.8	10
SHC	288	20.7	
Cucurbit[6]uril	298	46.4	11
MIL-101	303	2.9	12
[Zn ₄ (dmf)(ur) ₂ (ndc) ₄] (1)	273	15.3	<i>this work</i>
[Zn ₄ (dmf)(ur) ₂ (ndc) ₄] (1)	298	11.2	<i>this work</i>
[Zn ₁₁ (H ₂ O) ₂ (ur) ₄ (bpdc) ₁₁] (2)	273	32.3	<i>this work</i>
[Zn ₁₁ (H ₂ O) ₂ (ur) ₄ (bpdc) ₁₁] (2)	298	15.8	<i>this work</i>

* The selectivity factors were estimated as the ratio between the gas uptakes at 1 atm.

References

- [1] S. A. Sapchenko, D. G. Samsonenko, D. N. Dybtsev, and V. P. Fedin, *Inorg. Chem.*, **2013**, *52*, 9702.
- [2] Z. Otwinowski and W. Minor, *Methods Enzym.*, **1997**, *276*, 307.
- [3] G. M. Sheldrick, *Acta Crystallogr., Sect. A Found. Crystallogr.*, **2008**, *64*, no. Part 1, 112–122.
- [4] A.L. Myers and J.M. Prausnitz, *AIChE Journal*, **1965**, *11*, 121.
- [5] R. Banerjee, A. Phan, B. Wang, C. Knobler, H. Furukawa, M. O’Keeffe and O. M. Yaghi, *Science*, **2008**, *319*, 939.
- [6] H. Deng, C. J. Doonan, H. Furukawa, R. B. Ferreira, J. Towne, C. B. Knobler, B. Wang and O. M. Yaghi, *Science*, **2010**, *327*, 846.
- [7] B. Wang, A. P. Côté, H. Furukawa, M. O’Keeffe and O. M. Yaghi, *Nature*, **2008**, *453*, 207.
- [8] G. Ortiz, S. Brandès, Y. Rousselin and R. Guilard, *Chem. - A Eur. J.*, **2011**, *17*, 6689.
- [9] Y. Zhao, H. Wu, T. J. Emge, Q. Gong, N. Nijem, Y. J. Chabal, L. Kong, D. C. Langreth, H. Liu, H. Zeng and J. Li, *Chem. - A Eur. J.*, **2011**, *17*, 5101.
- [10] G. Sethia, H. a. Patel, R. R. Pawar and H. C. Bajaj, *Appl. Clay Sci.*, **2014**, *91-92*, 63.
- [11] H. Kim, Y. Kim, M. Yoon, S. Lim, S. M. Park, G. Seo and K. Kim, *J. Am. Chem. Soc.*, **2010**, *132*, 12200.
- [12] K. Munusamy, G. Sethia, D. V. Patil, P. B. Somayajulu Rallapalli, R. S. Somani and H. C. Bajaj, *Chem. Eng. J.*, **2012**, *195-196*, 359.
- [13] G. Kresse and J. Furthmüller, *Comput. Mater. Sci.*, **1996**, *6*, 15.
- [14] G. Kresse and J. Furthmüller, *Phys. Rev. B*, **1996**, *54*, 11169.
- [15] J. P. Perdew, K. Burke, and M. Ernzerhof, *Phys. Rev. Lett.*, **1996**, *77*, 3865.
- [16] P. E. Bloch, *Phys. Rev. B.*, **1994**, *50*, 17953.
- [17] G. Kresse and D. Joubert, *Phys. Rev. B*, **1999**, *59*, 1758.
- [18] H. J. Monkhorst and J. D. Pack, *Phys. Rev. B*, **1976**, *13*, 5188.
- [19] S. Grimme, *J. Comp. Chem.*, **2006**, *27*, 1787.
- [20] A. Kokalj, *Comput. Mater. Sci.*, **2003**, *28*, 155.
- [21] R. Matsuda, R. Kitaura, S. Kitagawa, Y. Kubota, R. V. Belosludov, T. C. Kobayashi, H. Sakamoto, T. Chiba, M. Takata, Y. Kawazoe, and Y. Mita, *Nature*, **2005**, *436*, 238.
- [22] D. N. Dybtsev, M. P. Yutkin, D. G. Samsonenko, V. P. Fedin, A. L. Nuzhdin, A. A. Bezrukov, K. P. Bryliakov, E. P. Talsi, R. V. Belosludov, H. Mizuseki, Y. Kawazoe, O. S. Subbotin, and V. R. Belosludov, *Chem. Eur. J.*, **2010**, *16*, 10348.
- [23] H. Sato, W. Kosaka, R. Matsuda, A. Hori, Y. Hijikata, R. V. Belosludov, S. Sasaki, M. Takata, and S. Kitagawa, *Science*, **2014**, *343*, 167.